ISSN 0965-545X, Polymer Science, Series A, 2022, Vol. 64, No. 5, pp. 456–466. © Pleiades Publishing, Ltd., 2022.
ISSN 0965-545X, Polymer Science, Series A, 2022. © Pleiades Publishing, Ltd., 2022.

MEDICAL POLYMERS

Citric Acid Cross-Linking of Chitosan Encapsulated Spearmint Oil for Antibacterial Cellulosic Fabric

Huma Tariq[a], Abdul Rehman[b,*], Farzana Kishwar[a], and Zulfiqar Ali Raza[c,]**

[a]*Department of Textile and Fashion Design, University of Home Economics, Lahore, Pakistan*
[b]*Institute of Microbiology and Molecular Genetics, University of the Punjab, Lahore, Pakistan*
[c]*Department of Applied Sciences, National Textile University, Faisalabad, 37610 Pakistan*
**e-mail: rehman_mmg@yahoo.com*
***e-mail: zarazapk@yahoo.com*

Received February 24, 2022; revised April 11, 2022; accepted May 10, 2022

Abstract—This study presents the encapsulation of spearmint oil (SMO) in chitosan microstructures prepared through the emulsion formation method. The SMO although is medicinally significant yet finds limited applications in medical and functional textiles because of its less stability and high volatility under ambient conditions. Nevertheless, its encapsulation in chitosan may enhance its stability and applicability for the said purpose. The SMO encapsulating chitosan microstructures were characterized using different analytical techniques and applied on cotton fabric through a green crosslinking of citric acid. The treated fabric revealed successful adhesion of microcapsules onto its surface confirmed via SEM and FTIR analyses. There observed a slight decrease in tensile strength of treated fabric; that, however, improved crease recovery behavior, and good antibacterial activity in response to broad-spectrum bacterial strains by reducing their 99% population; whereas, the stiffness of such fabric exhibited somehow increasing trend. Hence value-added multifunctional textiles produced, herein, may provide both surface and antibacterial activity for potential medical and healthcare applications without compromising their comfort properties.

DOI: 10.1134/S0965545X22700158

INTRODUCTION

Recently, immense progress in science and technology has facilitated the manufacturing of advanced textile materials and products with multifunctional properties. Such textiles are needed in homes, healthcare centers, and areas where hygienic protection is required without compromising their key performance properties. This, consequently, led to the development of some novel textiles having versatile properties such as antimicrobial activity, insect repellency, fragrance, skin softening, and moisturizing effects [1]. Among these, antimicrobial activity in textile materials is foremost needed in recent times. For instance, coronavirus and other infectious diseases have shown resilience towards the development of antibiotics, thus, the use of antimicrobial PPE increased manifolds [2, 3].

Synthetic antimicrobial agents including some metal particles, phenols, triclosan, organometallic compounds as well as quaternary ammonium compounds have been proven beneficial and active against a broad range of microbes with a provision of a durable and long-lasting impact on textile properties [4]. However, such antimicrobial agents may destroy the human skin resident bacteria too. Consequently, certain synthetic antimicrobial agents such as triclosan had been discouraged because of their toxicity and adverse effects [5]. On the safer side, non-toxic, and biodegradable antimicrobial agents are of utmost concern even after use thus supporting the conservation of the environment [6]. In the above context, natural antimicrobial agents are considered less toxic and more specific than synthetic ones thus being more accepted worldwide [7, 8]. Among various natural antimicrobial agents, essential oils have gained tremendous research interest, nowadays. They are rich in flavonoids, terpenes, alkaloids, and tannins contents which exhibit antimicrobial activity [9]. The active ingredients in most essential oils, however, are sensitive to light, moisture, aeration, and high temperatures. Therefore, a suitable approach is generally needed to protect them against degradation and unwanted release/evaporation. In this regard, encapsulation of essential oil is one of the most effective ways to increase their stability, and mask the taste, odors, and bio-activities [10]. In the above context, chitosan had been found a promising candidate as essential oils encapsulating matrix [11, 12].

The chitosan obtained from chitin's deacetylation possesses unique physicochemical and biological properties. It is one of the amplest found polysaccharides being an antimicrobial agent with profound

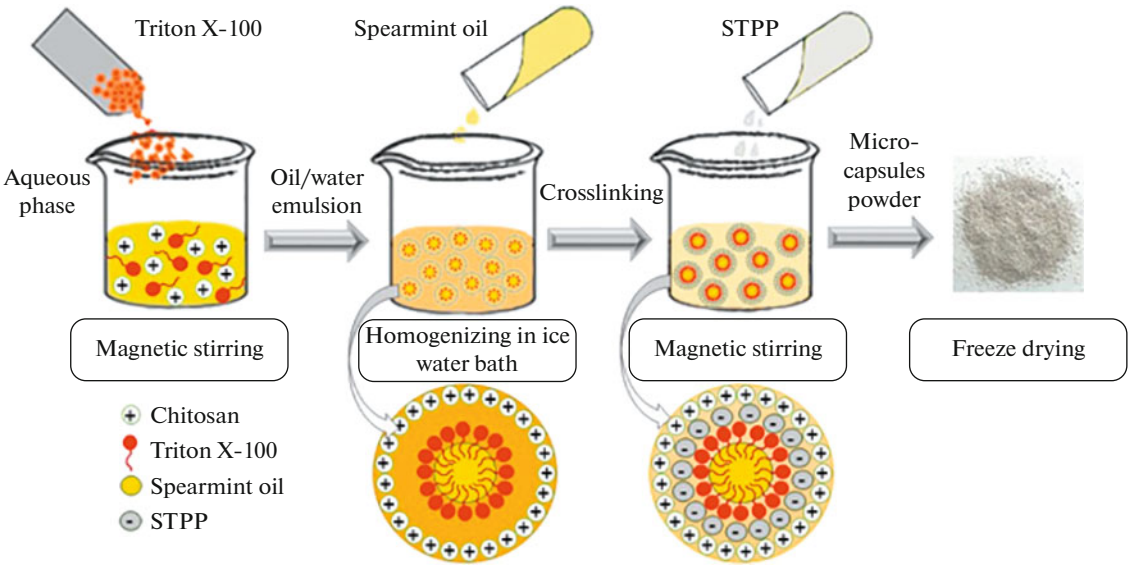

Fig. 1. Schematic illustration of the fabrication of chitosan encapsulated spearmint oil.

safety, nontoxicity, and biodegradability [13]. Chitosan-based microstructures, normally, do not establish a durable bond with the textile fabric, hence, a crosslinker is normally used for the said purpose [14]. Commonly employed crosslinkers such as formaldehyde or glutaraldehyde are found toxic causing harmful effects to the users and the environment [9]. Thus, alternative green crosslinkers like citric acid may be far more advantageous and appreciable to use.

The main objective of the present study was to develop chitosan micro-assemblies encapsulating spearmint oil (SMO) and their impregnation on cellulosic fabric using the green crosslinking strategy for antibacterial purposes. Both SMO encapsulating chitosan micro-assemblies and the treated fabrics were characterized, accordingly. To the best of our knowledge, so far, no work has been reported on the fabrication and application of SMO encapsulating chitosan micro-assemblies on cellulosic fabric via the green cross-linker of citric acid for desirable antibacterial and textile properties.

EXPERIMENTAL

Materials

Plain woven, bleached 100% cotton fabric with 117 GSM, 76 EPI, 68 PPI, and 64.47 CIE whiteness index (WI) was arranged from a local textile mill. Chitosan ($\bar{M}_w = (1–3) \times 10^5$, 90% degree of deacetylation) was procured from Bio Basic Inc., Canada, acetic acid and *n*-hexane from Sigma-Aldrich, Triton X-100 (an anionic surfactant), and sodium tripolyphosphate (STPP) from Bio M Laboratories, citric acid and sodium hypophosphite from Penta chemicals, and SMO from the local market.

Fabrication of Microcapsules

Chitosan (as 1 g) was dissolved in acetic acid (1%, w/v) through stirring for 2 h at room temperature. An appropriate amount of Triton X-100 was added and the contents were stirred at 500 rpm and 45°C for 30 min. The desirable amount of SMO (as 1, 2, or 3 wt %) was dissolved in *n*-hexane and poured into the chitosan solution. The contents were homogenized at 13000 rpm for 10 min on an ice bath to attain the oil/water emulsion. An aliquot of 50 mL of 0.4% (w/v) solution of STPP was dripped into the emulsion under agitation. Then the contents were centrifuged at 6500 rpm at 4°C for 15 min. The microcapsules were washed with distilled water to eliminate any untreated species, till pH 7 was achieved. Finally, it was ultrasonicated to achieve a homogenized suspension and finally freeze-dried overnight to obtain the required microcapsules for onward characterization. The above process has been sketched, accordingly (in Fig. 1).

Analytical Characterization

Microcapsular size distribution and zeta potential were measured using dynamic light scattering (DLS) analysis on a Zeta sizer, Malvern Instruments, UK. Surface morphologies of fabricated chitosan-based microstructures and the treated cotton fabric were examined under a scanning electron microscope (SEM from FEI Quanta 250) equipped with an energy dispersive X-ray (EDX) detector at an accelerating voltage of 20 kV for the elemental analysis. Any changes in any chemical functionalities during the formation and application of the microcapsules on the cellulosic fabric were investigated using an Attenuated Total Reflectance-Fourier transforms infrared (ATR-FTIR Bruker Tensor 27) spectroscope operated in the

wavelengths range of 500–4000 cm^{-1}. The crystal patterns of the test samples were recorded under an X'Pert PANalytical X-ray diffractometer in the 2θ range of 10°–60°.

Microcapsules Treatment of the Fabric

The pad-dry-cure method was used to apply the fabricated microstructures to the cotton fabric using citric acid as a crosslinker and sodium hypophosphite as the catalyst. The micro-capsular suspension (at 1–3%, w/w) was provided with citric acid (as 1%, w/v) and stirred for 30 min. Then the test fabric was immersed in it for 10 min and double padded at 70% wet pickup followed by drying at 110 ± 5°C for 2 min and finally curing at 170 ± 10°C for 2 min.

Textile Properties of the Fabrics

The textile characteristics of both treated and control fabric specimens were investigated using the standard testing methods. The WI was measured according to the standard method of AATCC 110 using a spectrophotometer (Color Eye 7000A, Gretag Macbeth). The crease recovery angle (CRA) of the test fabrics was measured using the standard test method of ISO 2313. The standard test of ASTM-D1388 was used to measure the stiffness of the test samples. The tensile strength of the fabric specimens was determined under the test method of ASTM-D-5035 using a tensile strength tester (Model KG-300). The tests were performed thrice and the results are the average of their readings. Analysis of variance (ANOVA) was done on the experimental data using SPSS® 21 software. The quantitative antibacterial activities of both untreated and treated fabric samples were measured using the standard test method of AATCC 100 against *Staphylococcus aureus* and *Escherichia coli* strains in terms of reduction in colony-forming units (CFU) using Eq. (1).

$$\text{Reduction in CFU } (\%) = \frac{\text{CFU in control} - \text{CFU in sample}}{\text{CFU in control}} \times 100. \quad (1)$$

Essential Oil Uptake and Release Profiles

Chitosan entrapped SMO micro-assemblies and the cotton fabric treated therewith were checked for the in vitro release of essential oil in the phosphate-buffered saline (PBS) at pH 7.4. For that purpose, the developed micro-assemblies (or the treated cotton fabric samples) were immersed in the PBS at the material to liquor ratio of 1 : 20 (w/v) under magnetic stirring at 500 rpm and room temperature for 72 h. Then the fabric samples were taken out (or the microcapsules were collected via centrifuging) and the remaining contents (or supernatant) were transferred to *n*-hexane (20 mL) and stirred, accordingly. The organic phase was separated using a separating funnel and hereafter evaporated by rotary evaporation for collecting any released oil contents in the media. Before that, the finishing contents (i.e., the SMO and chitosan) were checked by evaluating the weight differences between untreated and treated fabrics. For that purpose, ~ 0.1 g of test fabric was immersed in 5 mL of *n*-hexane and agitated for 3 h. Afterward, the fabric sample was dried and weighed to check for any release of finish.

RESULTS AND DISCUSSION

Chitosan Encapsulation of SMO

Herein, chitosan has been crosslinked via citric acid in the oil-in-water emulsion system in the presence of the anionic surfactant. The anionic surfactant, above its CMC, orients itself in such a way that its polar moieties form the outer layer of the micelles where the polar functionalities of the chitosan form the shell of the microcapsules; whereas, the oil phase is confined over the inner layer of anionic surfactant, being nonpolar, which ultimately form the core of the microcapsules (some illustrations have been shown in Fig. 1). The chitosan molecules were further crosslinked using STPP as a cross-linker across the chitosan chains.

The size distribution and zeta potential values of hence formed chitosan-based microstructures were measured using the DLS analysis (Fig. 2). The control chitosan microcapsules without any oil incorporation expressed a z-average of 250 ± 10 nm with the respective *z*-potential of +50 ± 5 mV. The z-average of chitosan microcapsules had been reported as 223 nm in the literature [15]. On incorporating SMO in the chitosan microcapsules, the z-average reduced to 180 ± 20 nm depending on the oil contents which could be attributed to the hydrophobic interactions (e.g., London dispersion forces) across the non-polar ends of essential oil and that of surfactant molecules. This resulted in the penetration of the hydrophobic ends of the surfactant molecules into the oil phase, at the core of the micelle, causing an overall reduction in microcapsules' size. The zeta potential usually expresses the surface charge and dispersion stability of the nanospheres. In the case of SMO encapsulating chitosan microcapsules, the zeta potential ranged from +20 ± 1 to +45 ± 5 mV depending on the oil contents in the finish. Generally, on increasing the SMO contents in the chitosan-based microcapsules from 1 to 3% (v/v), the zeta potential of the microcapsules increased, accordingly, thus making them more dispersible. This could be attributed to adequate electrostatic interactions between the shell of chitosan and the core of SMO in the microcapsules [14]. The microcapsules with the zeta potential above +30 mV are considered

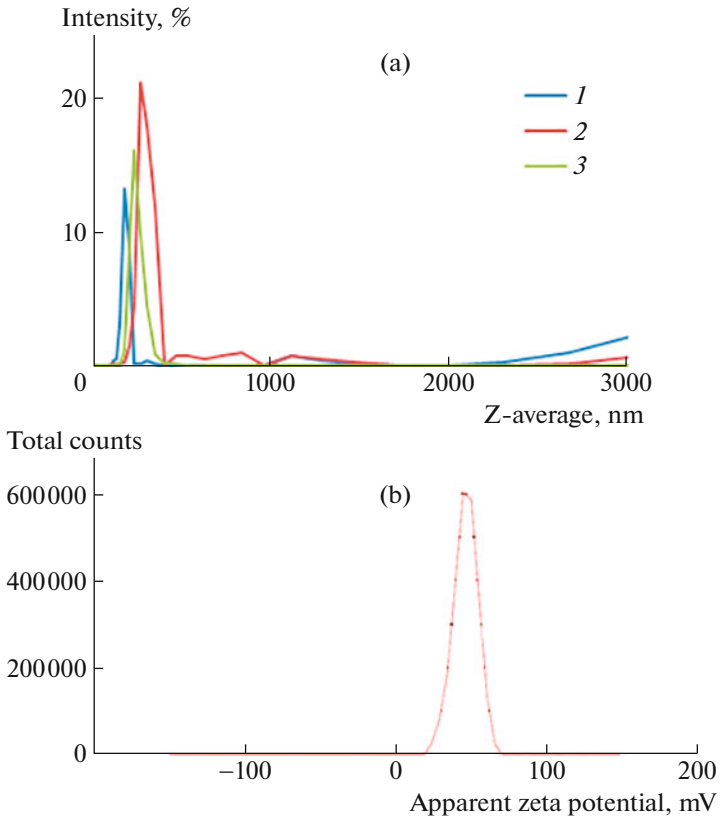

Fig. 2. (a) Z-average distribution of chitosan microcapsules at various SMO loadings: (*1*) 1, (*2*) 2, (*3*) 3%, and (b) zeta potential of chitosan microcapsules at 3% (w/w) SMO.

stable in the case of lyophobic sols; however, may be suitable below this value for lyophilic sols [16]. The polydispersity index (PDI) expresses the uniformity of particle size distribution. The PDI approaching 1 indicates maximum polydispersity, for instance in biomacromolecules, and approaching zero expresses monodispersity, usually with simple metal nanoparticles [15]. The PDI of SMO encapsulating chitosan microcapsules ranged from 0.36 to 0.39 indicating stable and regular size distributions of the prepared microcapsules.

The FTIR analysis of pristine chitosan powder, control chitosan microcapsules and 3 (%, w/w) SMO encapsulated chitosan microcapsules were conducted and the results are shown in Fig. 3a. The FTIR spectrum of pristine chitosan revealed some absorption peaks at 1645 and 1592 cm^{-1} associated with C=O stretching of amide I and amino group in the acetylated ring of chitosan macromolecule, respectively. Some other peaks at 1376 and 1056 cm^{-1} were linked to –OH bending and C–O–C stretching, respectively [17]. The control chitosan microcapsules showed C–H stretching at 2977 cm^{-1} and some characteristics peaks at 1600 and 1018 cm^{-1} for the amide group and C–O–C links, respectively. The FTIR spectrum of SMO (3%, w/w) incorporated chitosan microcapsules showed the presence of alcoholic, ethers anhydride, carboxylic acid, esters, and alkanes moieties which could be attributed to the complex composition of the essential oil. The inclusion of SMO in the chitosan microcapsules resulted in a significant increase in the C–H stretching at 2921 cm^{-1} revealing increased ester contents. The results are in close agreement with that already reported, where a peak at 2927 cm^{-1} had been observed with the inclusion of essential oil into the chitosan microcapsules [17].

Figure 3b shows the XRD spectra of pristine chitosan, control chitosan microcapsules and SMO (3%, w/w) encapsulated chitosan microcapsules. The pristine chitosan revealed a distinctive diffraction peak at the 2θ of 20.20°, which is attributed to the semicrystalline nature of the chitosan matrix [18]. The XRD spectrum of control chitosan microcapsules didn't show any distinctive peaks. The absence of this peak indicated that the STPP crosslinking decreased the chitosan crystallinity making it somewhat more amorphous [17]; whereas, the XRD spectra of SMO (3%, w/w) encapsulated chitosan microcapsules revealed the successful encapsulation of SMO and showed a peak at 2θ of 32.37°. This had been recorded by previous research, that the peak at 2θ of 31.0° was due to the inclusion of essential oil in the chitosan-based micro-

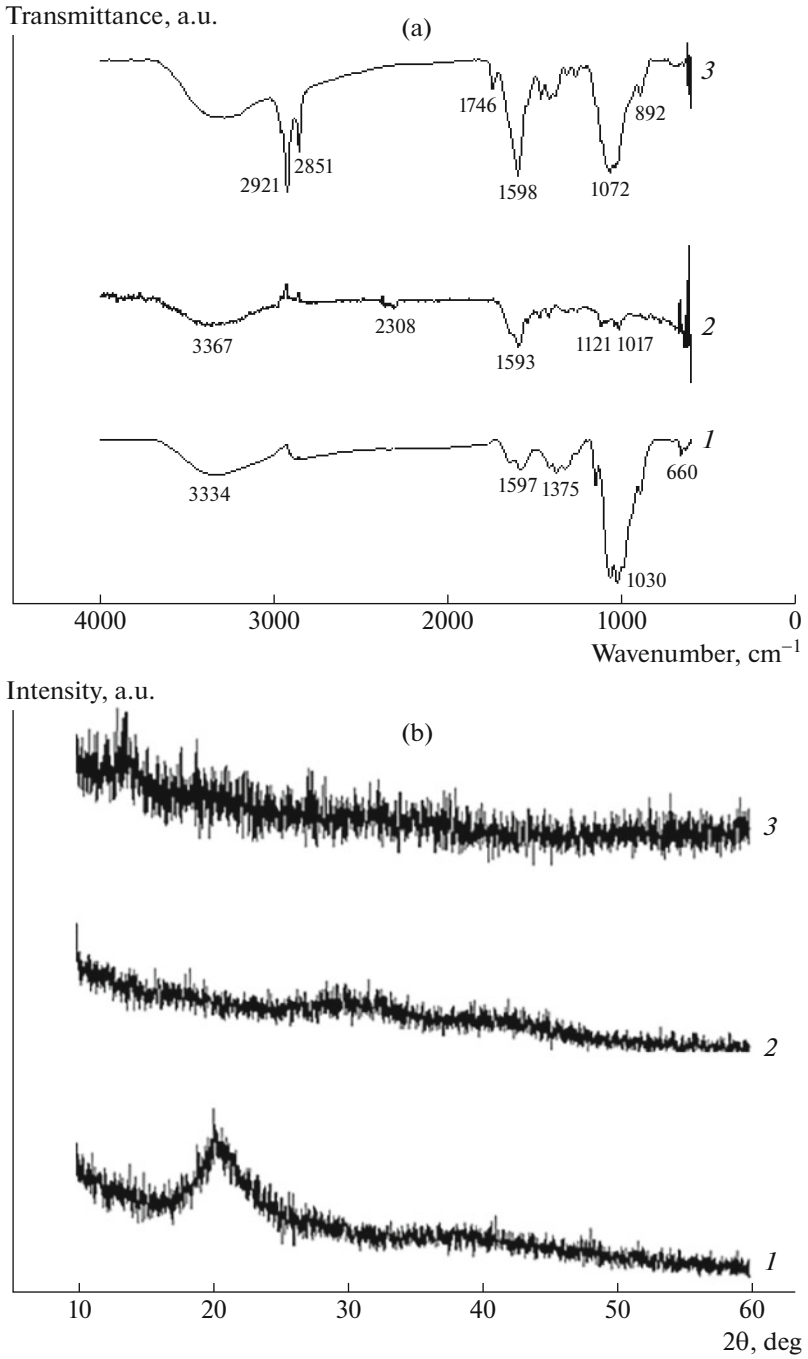

Fig. 3. (a) FTIR spectra and (b) XRD patterns of (*1*) pristine chitosan, (*2*) control chitosan microcapsules, and (*3*) SMO encapsulating chitosan microcapsules.

spheres [19]. The characteristic peak of chitosan became less intense because of oil loading into chitosan microcapsules towards reduced crystallinity of the chitosan-based microcapsules [18].

Characteristics of Treated Fabrics

Chitosan entrapped SMO microcapsules were anchored on the cotton fabric through the pad-dry-cure method in the presence of citric acid as the cross-linker; as mere chitosan-based finishes couldn't develop a strong attachment with the cotton fabric [14]. The chitosan microstructures in the presence of some dicarboxylic acids may develop durable cross-linking with the cellulose chains [20] through an esterification reaction occurring across them [21] in the presence of sodium hypophosphite as the catalyst. The

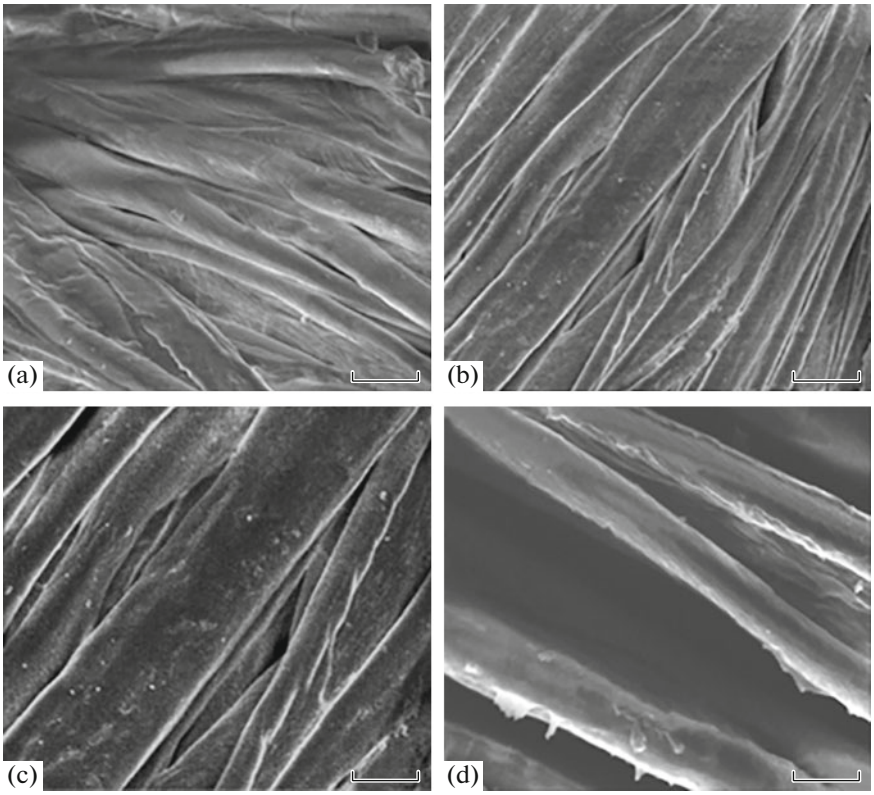

Fig. 4. SEM images of (a) pristine chitosan (C 25 wt %, O 54 wt %), (b) control chitosan microcapsules (C 44.5 wt %, O 53.0 wt %, N 1.5 wt %), and SMO encapsulating chitosan microcapsules treated cellulosic fabric (c) before washing and (d) after washing (C 45.0 wt %, O 53.1 wt %, N 1.4 wt %); bar = 10 μm.

fabric treated with microcapsules was characterized by surface chemical and textile properties.

Surface Morphology

The SEM micrographs of untreated fabric, control chitosan microcapsules treated and SMO incorporated chitosan microcapsules treated cotton fabrics showed successful impregnation of microcapsules there as shown in Fig. 4. The treated fabrics showed roughened surfaces in comparison to untreated fabric confirming the adhesion of microcapsules; whereas, a smooth surface texture was observed in the case of untreated fabric. The SEM image of the treated specimen after five standard washes indicated a durable attachment of the chitosan-based microcapsules on the fabric surface. The EDX analysis also confirmed the presence of nitrogen-containing finish, herein chitosan-based microcapsules, on the fabric surface (Fig. 4). The elemental analysis confirmed the absence or presence of SMO encapsulating chitosan microcapsules on the untreated or treated cellulosic fabrics. In the case of untreated cotton, carbon (C) and oxygen (O) were detected; whereas the SMO encapsulating chitosan microcapsules-treated cotton fabric showed the presence of nitrogen (N) too even after washing.

FTIR Analysis

The FTIR spectra of untreated fabric, control chitosan-treated cotton, and chitosan entrapped SMO-treated fabrics are shown in Fig 5. In the case of an untreated fabric sample, an absorption peak was observed at 3330 cm^{-1} due to the presence of hydroxyl groups in the cellulosic structure. A characteristic peak at 2946 cm^{-1} was indicated because of C–H stretching in the polymer backbone. Furthermore, another peek was appeared at 1159 cm^{-1} due to C–O–C stretching. The control chitosan microcapsules treated cotton sample showed an absorption peak for an amino group of chitosan at 3280 cm^{-1} and another peak at 1427 cm^{-1} for CH_2–NH_2, which in literature had been reported at 1438 cm^{-1} [14]. The chitosan entrapped SMO-treated fabric showed a peak at 1720 cm^{-1} corresponding to the carbonyl group of the essential oil. There observed some peaks at 1595 and 1514 cm^{-1} due to =C–H stretching and –NH bending, respectively, indicating an amidation interaction between residual free amino groups of the chitosan and –COOH of the citric acid [22].

Textile Properties of Treated Fabrics

The CIE WI describes any changes in the whiteness of the treated fabric after the application of chitosan

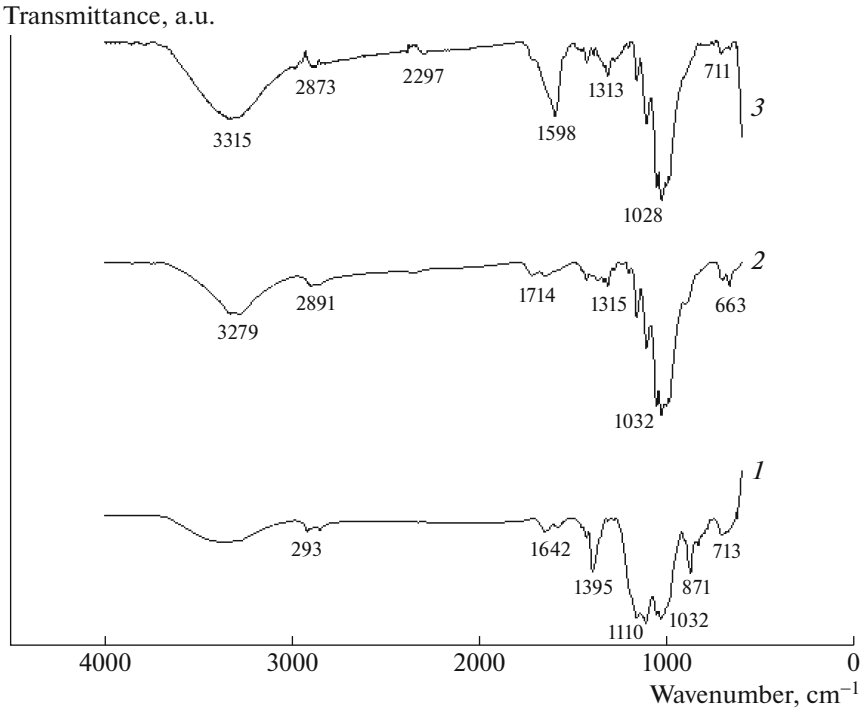

Fig. 5. FTIR spectra of (*1*) untreated, (*2*) chitosan microcapsules treated and (*3*) chitosan microcapsules containing SMO-treated cellulosic fabrics.

microcapsules. Herein, the untreated fabric expressed the WI of 64.47 CIE, and on treatment with chitosan microcapsules, it reduced to 59.27 CIE (Fig. 6a). Whereas, the inclusion of SMO1—3% (w/w) caused slight yellowing of the treated cotton fabric, as the WI was reduced from 40.20 to 31.96 CIE. Similar findings had already been reported previously where the WI was decreased upon treating the non-woven cotton matrix with aloe vera oil microcapsules [23]. Slight changes in the WI may be attributed to the thermal curing of the chitosan layer on the treated fabric which could cause a yellowing effect [24]. The application of Artemisia Afraoil microcapsules could also reduce the WO of the treated fabric [25].

Creasing is one of the top most problems faced while handling cotton fabric after washing. The creasing occurs on the cotton fabric due to free hydroxyl groups present in its structure [26]. During creasing, the molecular chains of cotton fabric present in the amorphous area slip over each other and break the weak hydrogen bonding due to the stretching of cellulosic chains. Thus, some new hydrogen bonds are formed in the stretched texture and the cotton fabric develops some creases affecting its appearance. However, the cotton fabric treated with chitosan-trapped SMO microcapsules showed improved crease recovery behavior in the presence of citric acid as the crosslinker (Fig. 6b). This could be attributed to the sizing effect of the chitosan layer on the cotton fabric whereas citric acid entangled the molecular chains of cellulose by developing bonds with its –OH groups [26]. It had been reported that appropriate crosslinking and oil lubrication may improve the crease recovery behavior of the treated fabrics [27]. However, the concentrations of crosslinker should be optimized as its excess contents may affect the physicomechanical properties of the treated fabric [28, 29].

The bending length of cotton fabric after treatment with chitosan encapsulated SMO expressed an increasing trend which indicated enhanced stiffness in the treated fabrics (Fig. 6c). A similar finding had been reported on coating the cotton fabric chitosan which increased the stiffness of treated fabric [30, 31]. Our results are also in close agreement with earlier findings that on treating the cotton fabric with chitosan nanoassemblies encapsulating α-tocopherol, there observed increased bending length making the treated fabric slightly stiffer [14]. This could be attributed to the chitosan layer deposition on the surface of the cotton fabric which also might enhance the cross-linking of cellulosic texture resulting in increased bending length. Furthermore, the chitosan microcapsules could enter the spaces between the fabric matrix causing restrictions in the inter-fiber movements thus increasing the bending length [30].

The tensile strength of untreated, control chitosan treated and fabric treated with chitosan entrapped SMO microcapsules is presented in Fig. 6d. The tensile strength of the fabric slightly decreased upon treatment with control chitosan microcapsules or with

Table 1. ANOVA for textile properties of SMO loaded chitosan microcapsules treated fabric samples

Response	*df*	SS	MS	*F*-Value	*p*-Value
Whiteness index	2	811.46	405.73	23.90	0.04*
CRA (warp)	2	24.80	12.40	12.40	0.07
CRA (weft)	2	21.33	10.66	4.57	0.18
Bending length (warp)	2	0.58	0.29	87.20	0.01**
Bending length (weft)	2	0.06	0.03	9.20	0.09
Tensile strength (warp)	2	1386.13	693.06	1.40	0.41
Tensile strength (weft)	2	1520.00	760.00	760.00	0.01**

Note: df = degree of freedom; SS = sum of square; MS = mean square.

those containing SMO. This could be attributed to stiffness caused by the chitosan sizing effect which reduced its resilience to bend. Similar results had also been reported in the literature where the cotton fabric treated with *Moringa oleifera* oil containing finish attached through citric acid crosslinking [31]. A decrease in tensile strength may also be attributed to the crosslinking of cotton fabric, as it increases the rigidity of cellulose molecules thus reducing the mobility of cellulosic chains. Therefore, the reduction of polymer mobility subsequently stops the redistribution of applied stress and decreases the tensile strength [32].

The experimental data presented in Fig. 6 was analyzed statistically using ANOVA and the corresponding results have been expressed in Table 1. A p-value of ≤ 0.05, usually, designates that the test factor is significant. The results show that the tensile strength in the weft direction, bending length in a warp direction, and the WI values were found to be significant based on the respective p-value values as stated above. Other factors such as stiffness both in warp and weft directions and bending length in weft direction were found insignificant demonstrating that the SMO loaded chitosan microcapsules treatment of cotton fabric didn't affect the said textile and comfort properties.

Antibacterial Activity

The cotton fabric treated with chitosan microcapsules and SMO entrapped microcapsules were investigated for antibacterial activity against *S. aureus* and *E. coli* cultures. The untreated cotton fabric exhibited no antibacterial activity against the test strains; however, the treated cotton fabric caused lower CFU in the culture media. The untreated fabric showed no reduction in the CFU (Fig. 7a); whereas, the cotton fabric upon treatment with chitosan control microcapsules showed an 84% CFU reduction against *S. aureus* and 82% reduction against *E. coli* strains. Moreover, treating the cotton fabric with chitosan microcapsules entrapping the SMO (at 3%, w/w), showed a 99% reduction in the CFU against both *S. aureus* and *E. coli* strains (Fig. 7a). Thus, the results demonstrated that the chitosan encapsulating SMO-treated cotton fabric showed good board-spectrum antibacterial activity. Similarly, peppermint oil/water emulsion had been applied to cotton using an ionic binder to impart antibacterial efficiency near 98% against the *S. aureus* strain [33]. The antibacterial activity might be attributed to the hydrophobicity of the essential oil, which disrupts the lipid layer of the cell membrane causing leakage of essential cell components thus leading to bacterial death [15]. Furthermore, the positively charged amino groups of chitosan may interact with the negatively charged cell membrane and damage the latter thus leaching its cytoplasmic inclusions. This results in inhibiting the bacterial growth on the fabric surface as well as in the culture medium where chitosan might leach [34].

SMO Uptake and Release Profiles

The finishing contents (i.e., SMO and chitosan) were determined by measuring the weight difference between the untreated, control chitosan treated and chitosan encapsulating SMO-treated fabrics (Fig. 7b). Thereby, about 0.30 g chitosan per g of the treated fabric was recorded whereas 0.38, 0.57, and 0.78 g SMO contents per g of treated fabric were noted with the chitosan microstructures encapsulating SMO contents at 1, 2, and 3 (%, w/w), respectively. The SMO-loaded chitosan microstructures and therewith treated fabrics were examined for oil release profile in the PBS medium (Fig. 7c). It was found that 7 (%, w/w) of initial oil contents were released into the medium by immersing the SMO-loaded chitosan microcapsules in the medium for 24 h. Further after 72 h of immersion, 15.33 (%, w/w) oil contents were released into the medium. The results demonstrated a slow release of SMO from the treated fabric into the PBS medium. There observed 3.1 (%, w/v) release of SMO contents into the PBS at 24 h of immersion which then reached 10.3 (%, w/w) at 72 h. The coarse surface of cotton fabric possesses interspaces that might enable it to absorb microcapsules thus ensuring oil retention [35]. The release of SMO from the chitosan microcapsules could be due to diffusion of SMO along with swelling of chitosan microcapsules while interacting with the

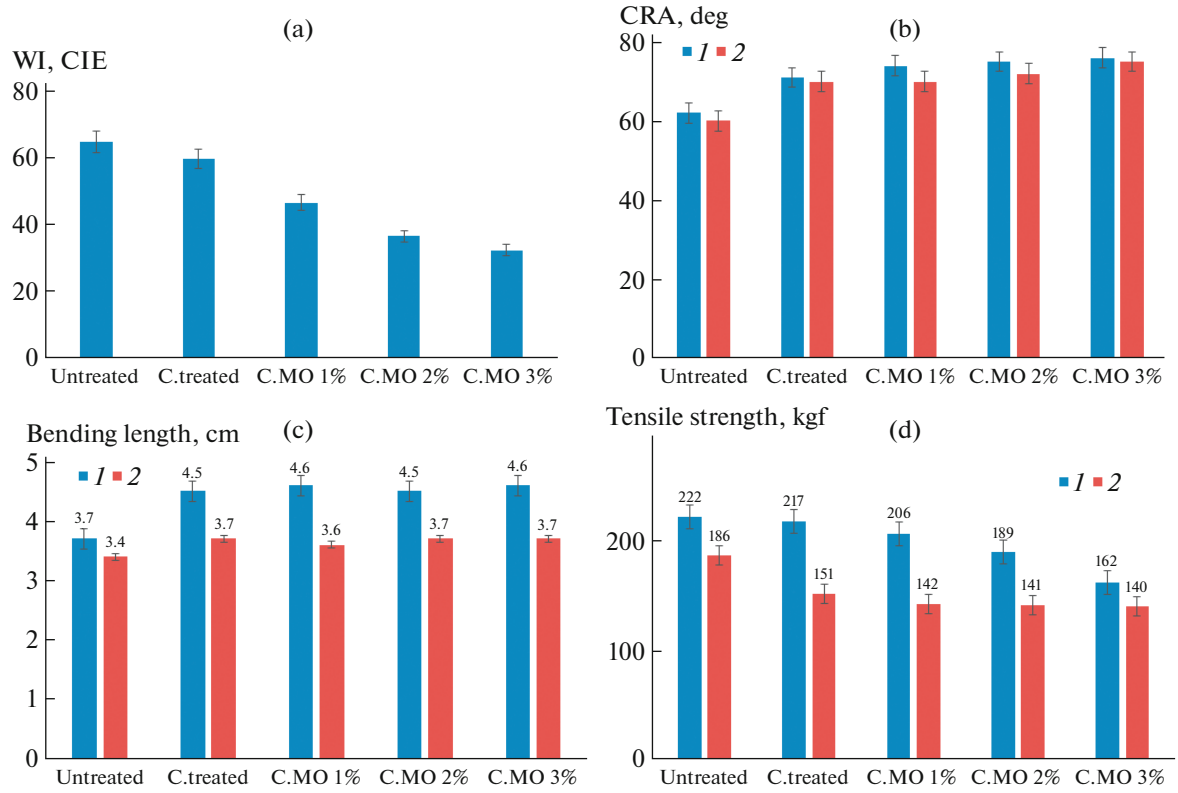

Fig. 6. (a) Whiteness index, (b) CRA, (c) bending length and (d) tensile strength ((*1*) warp and (*2*) weft) of untreated, and chitosan entrapped SMO-treated cellulosic fabrics (with 0 to 3% SMO contents from left to right).

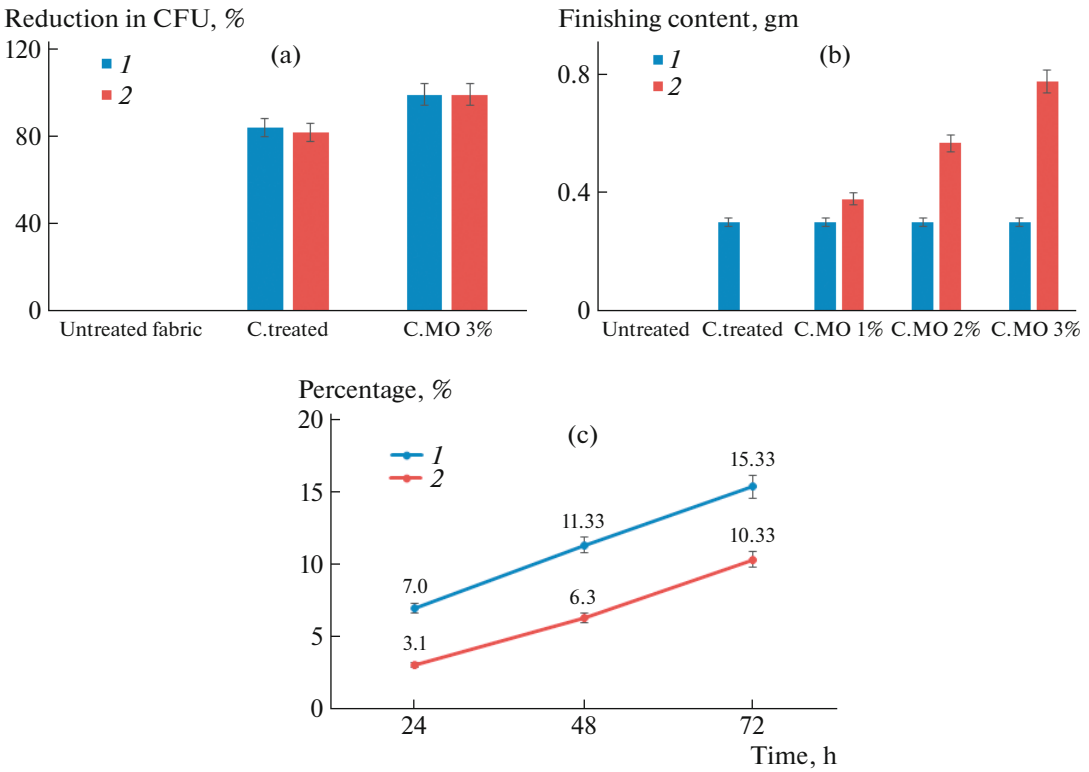

Fig. 7. (a) Antibacterial activity of treated and untreated fabrics: (*1*) *E. coli*, (*2*) *S. aureus*; (b) estimation of finishing contents loaded on the test samples. (*1*) Chitosan content, (*2*) spearmint oil content, and (c) SMO release profiles of (*1*) microcapsules and (*2*) the treated fabric, in phosphate-buffered saline of pH 7, dipped for the mentioned duration. The microcapsules contained initially 3% (w/w) SMO whereas the treated fabric was 0.7 mg SMO/g.

PBS medium [14]. It could be ascribed as an increase in osmotic pressure together with ion mobility could cause the microcapsules' swelling and the release of SMO into the PBS media.

The slow oil release from treated fabric could be attributed to the effective crosslinking of chitosan microstructures to cellulosic fabric through esterification using citric acid which resulted in a fewer number of hydroxyl groups available for interaction with the aqueous phase [27]. The crosslinking generally develops a three-dimensional network and acquires the hydroxyl groups of cellulose. Thus, it increased the hydrophobicity of the SMO/chitosan microcapsules treated fabric while decreasing the availability of water molecules to interact with the microcapsules resulting in a slower release of SMO from the treated fabric [14].

The results confirmed the successful impregnation of SMO-loaded chitosan microcapsules on the cotton fabric towards the sustained release of active ingredients for potential biomedical applications. Such a novel alternative finish exhibited good antibacterial activities against common bacterial pathogens found in hospital wards and on the PPE of the healthcare staff thus further validating its potential for biomedical textiles.

CONCLUSIONS

Presently, growing concerns for biosafety and toxicity of materials have prompted scientists to focus their attention on developing new methods for preserving bioactivity and bioavailability of active agents. Microencapsulation has been proven an efficient approach for this purpose. We report the successful and sustainable development, characterization, and application of SMO encapsulating chitosan microcapsules, using citric acid as the crosslinking agent onto the cellulosic textiles. Green cross-linking of citric acid with cellulosic fabric ensured the successful application of microcapsules on textile substrates without causing any toxicity and ensuring sustainability in textile manufacturing. The minimum z-average diameter of the oil-loaded microcapsules was achieved as 180 ± 20 nm with the optimum amount of encapsulated SMO. The surface morphology of treated fabrics became roughened in comparison to the untreated cellulosic fabric. The SMO-loaded chitosan microcapsules treated fabrics showed broad-spectrum antibacterial activity against common pathogens without significantly altering other textile properties such as tensile strength and stiffness. Moreover, such finished fabric exhibited improved crease recovery behavior and a wrinkle-free appearance. Lastly, even though numerous developments have been witnessed, in the future there is still a need for in vivo studies to explore its cytotoxicity against the human resident flora. Furthermore, the process could be investigated on large scale to achieve financial sustainability.

ACKNOWLEDGMENTS

H. Tariq and F. Kishwar appreciate the research facilities provided by the National Textile University, Faisalabad.

CONFLICT OF INTEREST

The authors declare that they have no conflict of interest.

REFERENCES

1. G. Natarajan, T. P. Rajan, and S. Das, J. Nat. Fibers **27**, 1 (2020).
2. D. Dridi, A. Bouaziz, S. Gargoubi, A. Zouari, F. B'chir, A. Bartegi, H. Majdoub, and C. Boudokhane, Coatings **1**, 980 (2021).
3. Z. A. Raza, M. Taqi, and M. R. Tariq, J. Text. Inst. **13**, 1 (2021).
4. M. Rastogi, S. Sharma, and S. Sharma, Asian J. Med. Sci. (Faisalabad, Pak.) **10**, 150 (2021).
5. B. Tawiah, W. Badoe, S. Fu, Fibres Text. East. Eur. **24**, 136 (2016).
6. A. Reshma, V. B. Priyadarisini, and K. Amutha, Int. J. Life Sci. Pharma Res. **8**, 10 (2018).
7. Y. B. Chong, H. Zhang, C. Y. Yue, and J. Yang, ACS Appl. Mater. Interfaces **10**, 15532 (2018).
8. J. V. Vastrad and S. A. Byadgi, Int. J. Curr. Microbiol. Appl. Sci. **7**, 284 (2018).
9. S. Karagonlu, G. Basal, F. Ozyildiz, and A. Uzel, Int. J. New Technol. Res. **3**, 1 (2018).
10. M. Mehran, S. Masoum, and M. Memarzadeh, Ind. Crops Prod. **154**, 112694 (2020).
11. S. Ghayempour and M. Montazer, J. Microencapsulation **33**, 497 (2016).
12. Z. A. Raza, U. Bilal, U. Noreen, S. A. Munim, S. Riaz, M. U. Abdullah, and S. Abid, Fibers Polym. **20**, 1360 (2019).
13. Z. A. Raza, S. Khalil, A. Ayub, and I. M. Banat, Carbohydr. Res. **492**, 108004 (2020).
14. Z. A. Raza, S. Abid, A. Azam, and A. Rehman, Cellulose **27**, 1717 (2020).
15. M. Hadidi, S. Pouramin, F. Adinepour, S. Haghani, and S. M. Jafari, Carbohydr. Polym. **236**, 116075 (2020).
16. S. Riaz, Z. A. Raza, and M. I. Majeed, Polym. Bull. **77**, 775 (2020).
17. A. Shetta, J. Kegere, and W. Mamdouh, Int. J. Biol. Macromol. **126**, 731 (2019).
18. S. Saber-Samandari and S. Saber-Samandari, Mater. Sci. Eng., C **75**, 721 (2017).
19. R. Bagheri, P. Ariaii, and A. Motamedzadegan, J. Food Meas. Charact. **15**, 1395 (2021).
20. M. Montazer and M. G. Afjeh, J. Appl. Polym. Sci. **103**, 178 (2007).
21. E. Sunder and G. Nalankilli, Int. J. Eng. Res. Technol. **3**, 1769 (2014).
22. F. A. Scacchetti, E. Pinto, and G. M. Soares, Procedia Eng. **200**, 276 (2017).

23. J. O. Fiedler, O. G. Carmona, C. G. Carmona, M. J. Lis, A. M. S. Plath, R. B. Samulewski, and F. M. Bezerra, J. Text. Inst. **111**, 68 (2019).

24. Z. Zhao, C. Hurren, M. Zhang, L. Zhou, J. Wu, and L. Sun, Materials **13**, 5365 (2020).

25. A. Azmeraw, S. Maiti, S. Biranje, and R. V. Adivarekar, in *Proceeding of 8th International Conference on Cotton, Textile and Apparel Value chain in Africa (CTA-2019), Bahir Dar, Ethiopia, 2019* (Bahir Dar, 2019), p. 129.

26. Z. A. Raza, F. Anwar, I. Hussain, S. Abid, R. Masood, and H. Shahzad Maqsood, Pigm. Resin Technol. **48**, 169 (2018).

27. B. Stefanovic, M. Kostic, M. Bacher, T. Rosenau, and A. Potthast, Text. Res. J. **84**, 449 (2014).

28. A. A. Mukthy, A. Yousuf, and M. Anwarul, Int. J. Sci. Eng. Technol. **990**, 983 (2014).

29. S. Abid, T. Hussain, A. Nazir, Z. A. Raza, A. Siddique, A. Azeem, and S. Riaz, Clothing Text. Res. J. **36**, 119 (2018).

30. G. Dhiman and J. N. Chakraborty, Fashion Text. **2**, 1 (2015).

31. G. Gebino, G. Ketema, A. Fenta, G. K. Rotich, and A. Debebe, Res. J. Text. Apparel **25**, 240 (2021).

32. W. Ye, J. H. Xin, P. Li, K.-L. D. Lee, and T.-L. Kwong, J. Appl. Polym. Sci. **102**, 1787 (2006).

33. P. Wankhade, N. Mehra, and V. Gotmare, in *Functional Textiles and Clothing 2020* Ed. by A. Majumdar, D. Gupta, and S. Gupta (Springer, Singapore, 2021), p. 149).

34. C. Prapruddivongs and N. Sombatsompop, Adv. Mater. Res. **747**, 111 (2013).

35. Y. Li, L. Ai, W. Yokoyama, C. F. Shoemaker, D. Wei, J. Ma, and F. Zhong, J. Agric. Food Chem. **61**, 13 (2013).